



Development of Hazard Consistent Fragility Functions for RC Shearwall Buildings in Southwestern BC

Mike Fairhurst¹, Armin Bebamzadeh², Carlos E. Ventura³

¹ Ph.D. Student, Department of Civil Engineering, University of British Columbia - Vancouver, BC, Canada.

² Research Associate, Department of Civil Engineering, University of British Columbia - Vancouver, BC, Canada.

³ Professor, Department of Civil Engineering, University of British Columbia - Vancouver, BC, Canada.

ABSTRACT

This paper investigates the collapse risk of reinforced concrete (RC) coupled shearwall buildings in Southwestern BC – a region dominated by three distinct earthquake sources: crustal, subduction intraslab, and subduction interface. This paper uses incremental dynamic analysis (IDA) of an 18 storey RC concrete building model under three suites of ground motions – one suite for each unique earthquake source – to develop fragility curves for each source type. The suites are developed using conditional spectra (CS), such that the amplitude, shape, and variation in the suite spectra are consistent with the hazard type. A novel algorithm involving spectral matching was used to match the subduction intraslab and interface events to their CS. The results indicate that subduction interface events are the most demanding for this type of structural system, followed by crustal, and then intraslab. This is due to both the spectral shape of the anticipated ground motions and the shaking characteristics of each source (e.g. duration).

Keywords: RC concrete shearwall buildings, subduction megathrust earthquakes, conditional spectra, ground motion duration, nonlinear time history analysis.

INTRODUCTION

The seismicity in Southwestern BC is dominated by the subduction of the oceanic Juan de Fuca plate beneath the continental North America plate occurring about 100 km west of Southern Vancouver Island – also called the Cascadia Subduction Zone. The seismic hazard in this region includes contributions from three sources: shallow crustal events, which occur along shallow faults in the Earth's crust; subduction intraslab events, which occur deep within subducting tectonic plates; and subduction interface events, which are caused by slip between subducting tectonic plates. Geophysical parameters and structural response can vary substantially between these types of earthquakes.

Crustal and subduction intraslab events are typically lower magnitude (<8) and have a short shaking duration. Subduction interface events can be much larger (up to magnitude 9 [1]) with much longer durations of strong shaking. Several recent studies have shown that different structural systems are more susceptible to damage and collapse when subjected to longer duration motions, even when compared to shorter motions of equal intensity (typically characterized through spectral values) [2-5]. Subduction interface records also tend to have a different spectral shape than crustal or intraslab events, with less response in the shorter periods and more in the longer periods.

In this study, a novel algorithm is used to produce suites of hazard-consistent ground motions representing the crustal, intraslab, and subduction interface hazards in Vancouver, BC. These suites are then used to run incremental dynamic analyses (IDA) on an 18 storey coupled RC shearwall building model. The model uses fiber elements and rotational hinges to capture the nonlinear behavior of the structure, including cyclic and in-cycle degradation. Modeling of this degradation as well as second order (P-Delta) effects is essential to capture the full effect of ground motion duration. The IDA results are used to develop fragility curves for this type of building, for each type of motion.

NUMERICAL MODEL

Archetype Building

The building modeled for this study was an 18 storey reinforced concrete shearwall building, typical of an existing residential building in Vancouver, BC. The lateral load resisting system includes three interior reinforced concrete shearwalls which comprise the elevator and stair core of the building. The gravity resisting system of the building includes circular perimeter

and interior columns and 8" slabs at each story. The floor area is about 5200 ft² per story and the weight was calculated as 0.21 kips/ft² (approximately 10 kN/m²). The floor plan is illustrated in Figure 1a.

The building was designed using the equivalent lateral force procedure (ELFP) for a base shear calculated in accordance with the 2010 National Building Code of Canada (NBCC) for Vancouver, BC based on conventionally constructed coupled walls [6]. The seismic force reduction factor (R_dR_o) of this system is 1.95. Reinforcement in the shearwalls for building is illustrated in Figure 1b. The walls are connected by 2' deep header beams which are reinforced by transverse 15M stirrups spaced at 4".

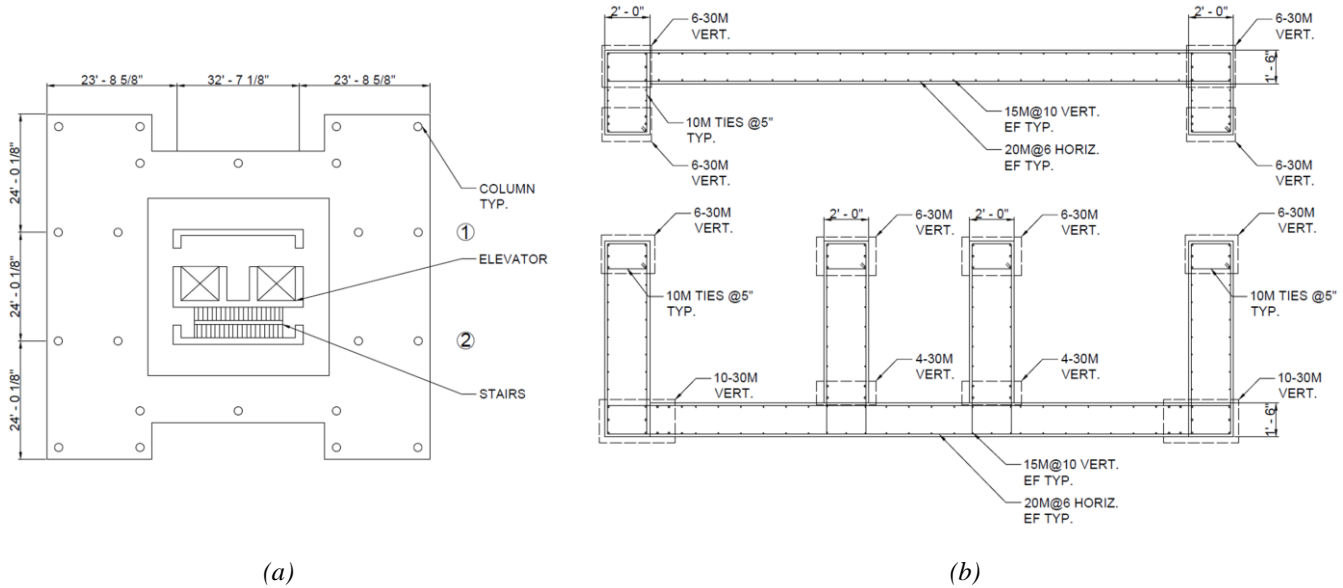


Figure 1. Archetype building a) floor plan, and b) shearwall reinforcement

Numerical Model

The OpenSees framework [7] was used to develop a numerical model for the archetype building following Fairhurst et al. [4]. The interior shearwalls were modeled using fiber elements with a displacement-based formulation and elastic shear hinges to capture elastic shear deformations. The elastic shear hinges had a stiffness reduced to 0.1 times their elastic stiffness to account for cracking [8].

The header beams were modeled using elastic beam elements to with nonlinear shear hinges to account for the shear yielding and nonlinearity in the elements. The elastic beam elements were modeled considering a cracked section modulus ($I_{cracked} = 0.35I_{gross}$) [9].

The nonlinear shear hinge properties were calibrated to a reverse-cyclic test on a similar beam performed by Galano and Vignoli [10] using the Pinching4 material model [11]. This model is able to capture capture pinching, in-cycle degradation, and cyclic stiffness and strength degradation. A comparison of the test results to the calibrated Pinching4 material model is presented in Figure 2a.

Concrete was modeled using the Concrete02 material model in OpenSees [12]. Confinement was accounted for using the Mander et al. relationship [13]. Both crushing and spalling are captured in this material model. Reinforcing steel was modeled using the ReinforcingSteel material model which can account for cyclic fatigue [14]. Buckling and fracture of the reinforcement was captured through the use of the MinMax material. To do this, the MinMax material was set to return zero strength and stiffness when the strain in the steel material reached the concrete crushing strain (assuming steel buckling will occur immediately after the surrounding concrete crushes) or the steel fracture strain [8]. Bar slip was modeled using a zero length fiber section at the base of each wall using the Bond SP01 material model for the steel bars following Zhao and Sritharan [15].

To account for the second order effects of the weight carried by the gravity system a leaning (or P-Delta) column was included in the model. The weight of the structure not applied directly on the shearwalls was applied on the leaning column. Rigid diaphragm constraints were applied at each level.

Damping was applied as 2.5% Rayleigh damping in the first and third modes. The first three periods of the model were 1.71, 0.51, and 0.26 s. An illustration of the OpenSees model is presented in Figure 2b.

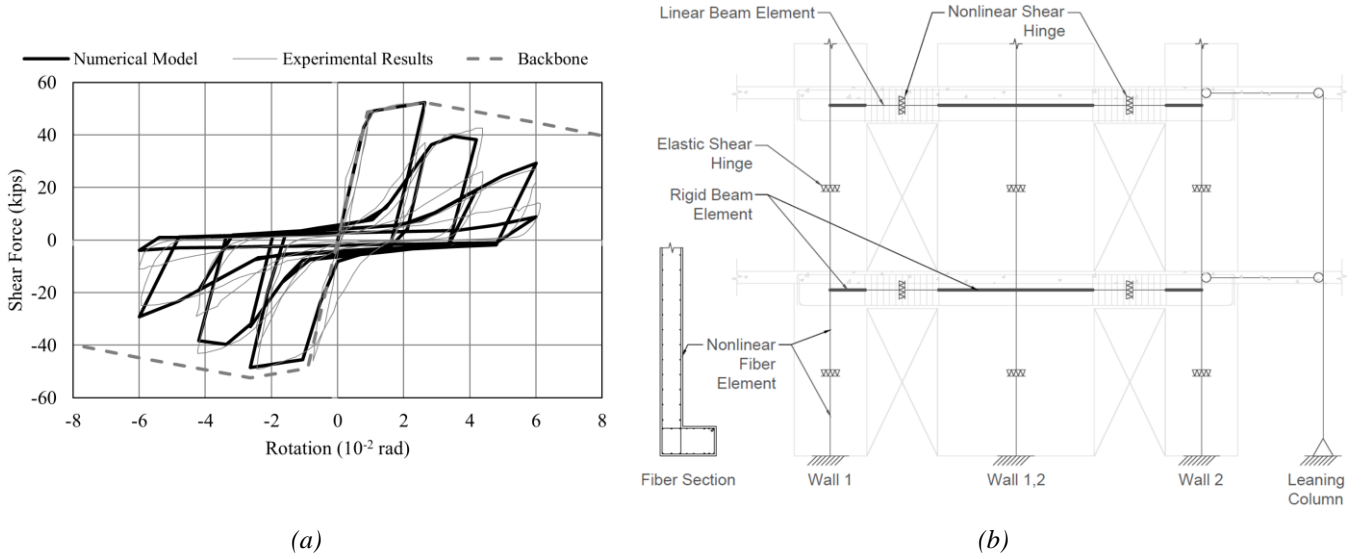


Figure 2. a) Nonlinear shear hinge model for the header beams, and b) typical storey of the OpenSees model

GROUND MOTION SUITES

The following sections describe the development of the three ground motion suites. First the target conditional spectrum (CS) is introduced. Next, the methodology to match each CS and resulting ground motion suites are described.

Target Conditional Spectra

A CS is a scenario- and period-dependent response spectrum and is computed using seismic hazard deaggregation information obtained from traditional probabilistic seismic hazard analysis (PSHA) [16]. A CS is recommended for risk-based assessments and collapse analysis as it properly targets both the mean and the variation of the spectrum [17]. Accordingly, a CS was developed for each motion type based on the 2015 Geological Survey of Canada (GSC) seismic hazard model [18].

From Lin et al. [16], the mean of a CS, conditioned at period T_c , for each period, T : $\mu_{\ln SA | \ln SA(T_c)}(T)$; is computed as:

$$\mu_{\ln SA | \ln SA(T_c)}(T) = \mu_{\ln SA}(M, R, \theta, T) + \rho(T, T_c) \cdot \varepsilon(T_c) \cdot \sigma_{\ln SA}(M, R, \theta, T) \quad (1)$$

Where $\mu_{\ln SA}(M, R, \theta, T)$ is the mean logarithmic spectral acceleration predicted by an appropriate ground motion prediction equation (GMPE) for T_i based on a scenario-specific magnitude: M , distance metric: R , and any other number of parameters: θ ; $\rho(T, T_c)$, is the epsilon correlation coefficient between T and T_c ; $\sigma_{\ln SA}(M, R, \theta, T)$ is the lognormal standard deviation from the GMPE for the specified scenario; and $\varepsilon(T_c)$ is the epsilon value at the T_c , for the specified hazard level, computed as:

$$\varepsilon(T_c) = \frac{\ln(SA(T_c)) - \mu_{\ln SA}(M, R, \theta, T_c)}{\sigma_{\ln SA}(M, R, \theta, T_c)} \quad (2)$$

Where $SA(T_c)$ is the spectral acceleration required at the conditioning period for the specific hazard level, and all other terms have previously been defined. For example, $SA(T_c)$ may be the spectral acceleration with an annual exceedance frequency (AEF) of 1/2475 at T_c . Then, M , R , and θ would come from a seismic hazard deaggregation for this spectral value at T_c .

The target logarithmic standard deviation at each period, $\sigma_{\ln SA | \ln SA(T_c)}(T)$, of the CS is computed as:

$$\sigma_{\ln SA | \ln SA(T_c)}(T) = \sigma_{\ln SA}(M, R, \theta, T) \cdot \sqrt{1 - \rho^2(T, T_c)} \quad (3)$$

For this study, the CS were conditioned at $T_c = 1.75$ s to the 1/2475 spectral acceleration ($SA(T_c = 1.75) = 0.277g$) for Vancouver, BC, Site Class C, obtained using the 2015 GSC seismic hazard model. The epsilon correlation coefficients developed by Baker and Jayaram [19], which have been observed to be suitable for both crustal and subduction events [20-22], were adopted. The target lognormal standard deviation was based on the constant (for all sources) GSC 2015 GMPE standard deviation model.

The conditional mean spectrum (CMS) for each source is illustrated in Figure 3a. Figure 3b shows the target lognormal standard deviation (constant for all sources).

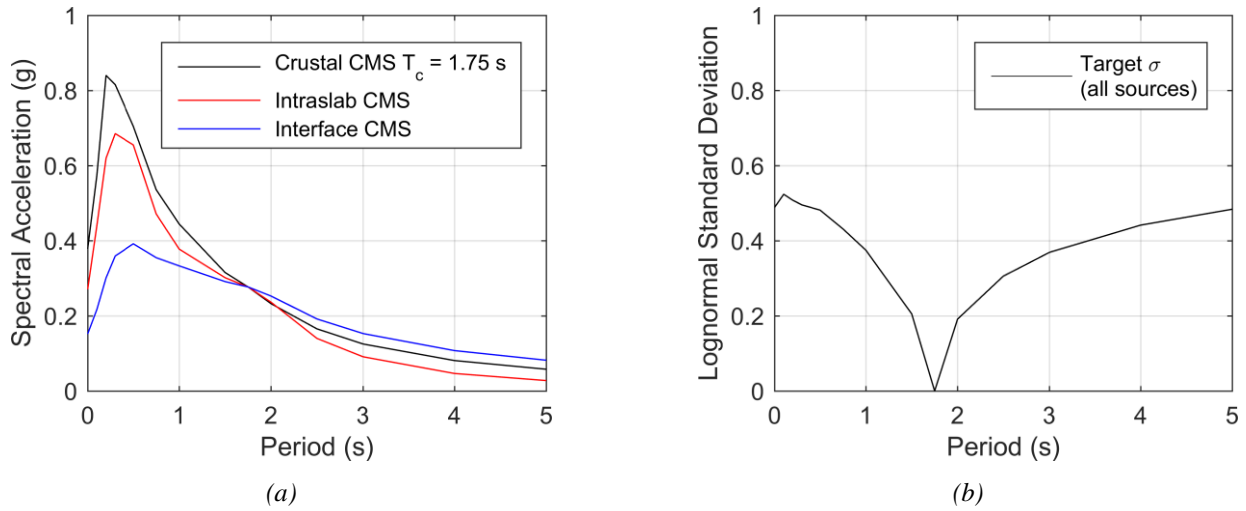


Figure 3. Target: a) CMS ($T_c = 1.75$ s) for each source; and b) lognormal standard deviation

Crustal Suite Development

The crustal suite was matched to the target CS (mean and standard deviation) using the algorithm by Jayaram et al. [23]. Records were selected from the PEER NGA West2 database [24]. NEHRP Site Class C records were selected from magnitude 5.5-7.5 events recorded at 0-80 km based on deaggregation results at $SA(T_c = 1.75) = 0.277g$. The selected crustal records are listed in the first column of Table 1.

The records were scaled at the conditioning period $T_c = 1.75$ s, which is approximately the first mode period of the model $T_1 = 1.71$ s. The period range of interest for selecting records (where the mean squared error, MSE, was minimized) was $0.1 \cdot T_1 \approx 0.2$ s to $2.0 \cdot T_1 \approx 3.5$ s (unshaded area in Figure 4).

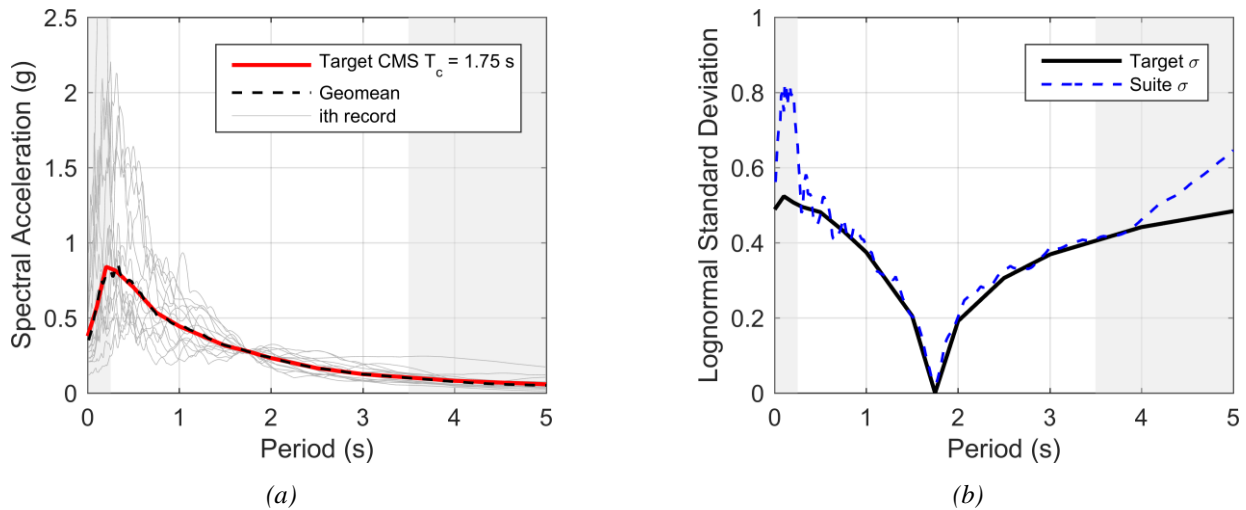


Figure 4. Crustal suite summary: a) suite spectrum; b) suite lognormal standard deviation vs. target

Table 1. Selected Record Summary

Crustal				Intraslab				Interface			
Earthquake	Mag	Year	Station	Earthquake	Mag	Year	Station	Earthquake	Mag	Year	Station
Chi-Chi	6.2	1999	CHY029-N	Nisqually	6.8	2001	1437a-270	Maule	8.8	2010	LaFlorida-EW
Chi-Chi	6.2	1999	TCU-116	Nisqually	6.8	2001	0725a-270	Maule	8.8	2010	Penalolen-EW
Northridge	6.69	1994	5108-360	Geiyo	6.4	2001	EHM008-EW	Maule	8.8	2010	Matanzas-T
Coalinga	6.36	1983	COW-000	Nisqually	6.8	2001	1416a-125	Maule	8.8	2010	Hualane-T
Loma Prieta	6.93	1989	HSP-000	Michoacan	7.1	1997	UNIO-S90E	Maule	8.8	2010	SJCH-360
Tabas	7.35	1978	TAB-LN	Michoacan	7.1	1997	VILE-S90E	Tohoku	9.1	2011	CHB013-NS
Chi-Chi	6.2	1999	TCU070-N	Geiyo	6.4	2001	EHM005-EW	Tohoku	9.1	2011	AOM021-EW
Tabas	7.35	1978	DAY-LN	Geiyo	6.4	2001	EHM003-EW	Tohoku	9.1	2011	YMT002-EW
Cape Mendoza	7.01	1992	FOR-000	Ferndale	6.55	2010	1725-360	Tohoku	9.1	2011	AKT018-NS
Chi-Chi	6.2	1999	CHY034-N	Pingtung	6.94	2006	KAU081-N	Tohoku	9.1	2011	MYG005-EW
Northridge	6.69	1994	FAI-095	Ferndale	6.55	2010	KCT-HNN	Tohoku	9.1	2011	AKT006-EW
Mammoth	5.91	1988	CVK-090	Hamanaka	6.9	2006	HKD075-EW	Hokkaido	8.3	2003	HKD129-EW
Landers	7.28	1992	LCN-260	Pingtung	6.94	2006	KAU043-N	Hokkaido	8.3	2003	HKD039-EW
Landers	7.28	1992	NPS-000	Olympia	6.7	1949	OLY-356	Hokkaido	8.3	2003	HKD105-EW
Duzce	7.14	1999	BOL-000	Iniskin	7.15	2016	HOM-BNE	Michoacan	8.1	1985	AZIH-N00W

Subduction Intraslab and Interface Suite Development

The S^2GM database [25], supplemented with additional subduction records from the K-Net Japanese record database [26], was used as a record source for the subduction intraslab and interface records. For the intraslab suite, records were limited to recordings on Site Class C sites with magnitudes of 5.5-7.5 and distances of 50-150 km based on deaggregation results at $SA(T_c = 1.75) = 0.277g$. Site Class C records at distances of 30-150 km from magnitude 8+ events were considered for the subduction interface suite development. These constraints led to very few suitable records from the database, especially when trying to limit multiple recordings from one earthquake. Accordingly, the methodology from Fairhurst et al. [27] to match a target CS was applied as follows:

- 1) Seed records with appropriate metadata (site class, distance, magnitude) were selected and scaled to the target CMS from the limited database (Table 1).
- 2) A period-dependent factor function: $FF(T)$, between the target CMS: $SA_{target}(T)$, and seed geomean spectra: $SA_{geo}(T)$, was computed:

$$FF(T) = \frac{SA_{target}(T)}{SA_{geo}(T)} \quad (4)$$

- 3) A variable target spectrum (VTS) [28]: $VTS_j(T)$, is computed for each record, j , by multiplying the record's seed spectrum: $SA_j(T)$, by the factor function at each period:

$$VTS_j(T) = FF(T) * SA_j(T) \quad (5)$$

- 4) Each $VTS_j(T)$ is modified by a single linear function in log-space to adjust the standard deviation of the suite at each period T , while leaving the mean unchanged:

$$\ln(VTS_j^*(T)) = \ln(VTS_j(T)) \cdot \frac{\sigma_{\ln SA | \ln SA(T_c)}(T)}{\sigma_{VTS}(T)} - \mu_{VTS}(T) \cdot \frac{\sigma_{\ln SA | \ln SA(T_c)}(T)}{\sigma_{VTS}(T)} + \mu_{\ln SA | \ln SA(T_c)}(T) \quad (6)$$

where $VTS_j^*(T)$ is the modified VTS for record, j , $\mu_{\ln SA | \ln SA(T_c)}(T)$ is the target CMS, $\sigma_{\ln SA | \ln SA(T_c)}(T)$ is the target CS lognormal standard deviation, $\sigma_{VTS}(T)$ is the lognormal standard deviation of the suite of $VTS_j(T)$ before modification; and $\mu_{VTS}(T)$ is the lognormal mean of the suite before modification.

- 5) Finally, each seed record is spectrally matched to its target $VTS_j^*(T)$. This was done using existing spectral matching techniques implemented in RSPMatch v05 [29]. The resulting suite of matched records will match both the target mean spectrum and target standard deviation.

The same period range as used for the crustal suite (0.2-3.5 s) was used for spectral matching the seed records to their individual target VTS_j^* . The resulting subduction intraslab and interface suite spectra are illustrated in Figure 5 and Figure 6, respectively. The seed records are listed in Table 1.

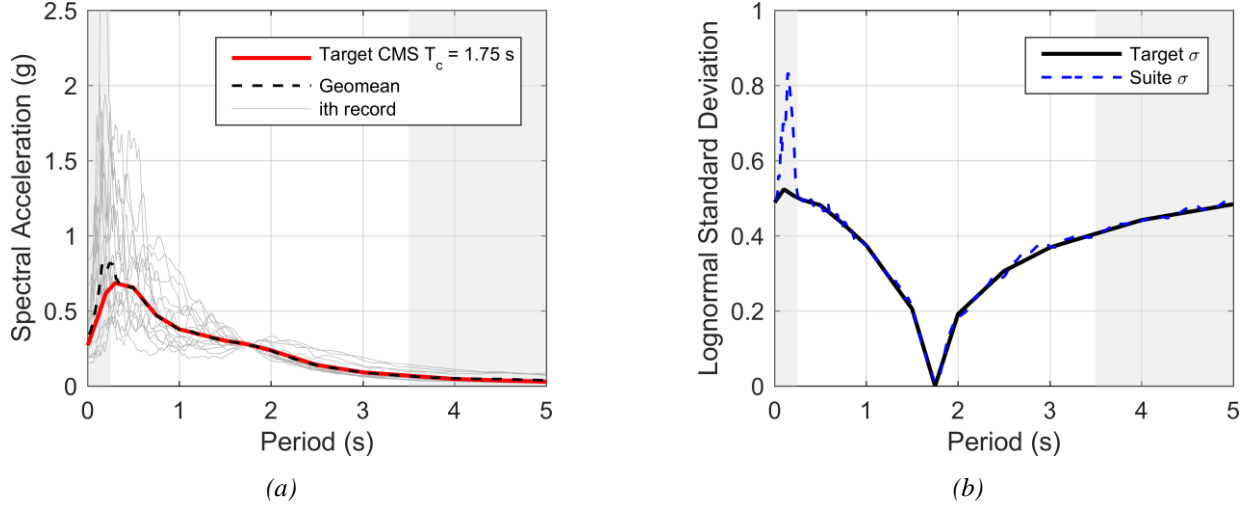


Figure 5. Subduction intraslab suite summary: a) suite spectrum; b) suite lognormal standard deviation vs. target

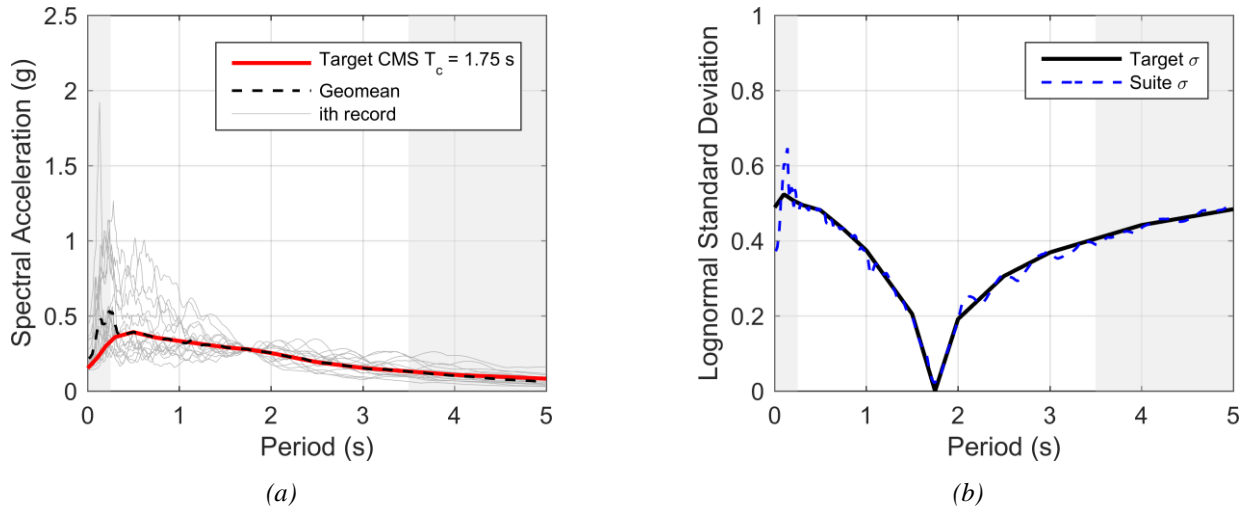


Figure 6. Subduction interface suite summary: a) suite spectrum; b) suite lognormal standard deviation vs. target

ANALYSIS RESULTS

Incremental dynamic analysis (IDA) was used to compute the fragility curves for the three motion suites. The three suites of ground motions were incrementally scaled and run using nonlinear time history analysis (NTHA) until collapse was detected. For this study collapse is defined as large interstory drifts (>5%). This drift limit was chosen because the gravity system, which was not explicitly modeled, is not expected perform past 5% drift, This is also slightly over the allowable maximum drift limit from LATBSDC of 4.5% [9] and past the drift where the IDA curves became flat.

The resulting fragility curves, expressed as both empirical functions and lognormal fitted functions, are presented in Figure 7. The median (expressed as a percent of the 2% in 5 year hazard level) and lognormal standard deviation values are presented in Table 2.

Table 2 and Figure 7 clearly show that the subduction interface suite was the most demanding, as it required the lowest scaling factors to reach collapse. Although the interface CS is much lower in the short periods, it was higher in the longer periods (see: Figure 3a), which may have led to more damage as the structures yielded and underwent period elongation. Also, the significant durations of the subduction suite records were, on average, much longer than the other two (76 vs. 12 s significant duration). This would have led to greater damage accumulation in the degrading nonlinear models. The crustal and intraslab results were similar – this is likely due to the similarity of both the CS (see: Figure 3a) and the nature of the ground motions (significant duration, pulses, etc.). The crustal CS was slightly higher than the intraslab CS across the period range – this is likely why the crustal suite was slightly more demanding (median collapse scaling level of 221 vs. 236%).

Table 2. IDA results: median collapse scaling level and lognormal standard deviation

	Crustal	Subduction Intraslab	Subduction Interface
Median Collapse Scaling Level (% of 2% in 50 year level)	221	236	181
Lognormal Standard Deviation	0.293	0.245	0.308

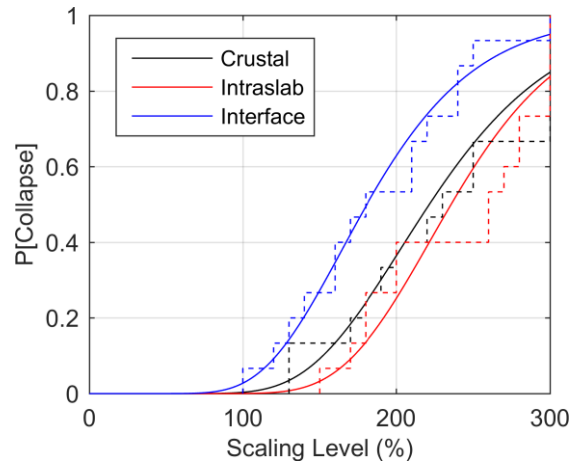


Figure 7. Resulting fragility curves for the three earthquake suites. Dashed lines represent the empirical CDF functions; solid lines represent the fitted function.

CONCLUSIONS

In this study three hazard-consistent suites of ground motions were developed for Southwestern BC and used to run IDA on a nonlinear degrading model of an existing RC concrete shearwall building typical of Vancouver, BC. The model was able to capture both nonlinear second order effects and all major modes of degradation for this structural system (concrete spalling, cracking and crushing; steel fatigue, buckling, slip, and rupture; and header beam cyclic and in-cycle degradation).

IDA results were used to develop fragility curves for each earthquake type. These curves demonstrate the vulnerability of this type of structure when subjected to the different types of potential ground motions and are useful for seismic risk and collapse assessment. The results showed subduction interface events to be the most demanding, due to both spectral shape and ground motion characteristics (e.g. duration). These results indicate that structures designed to national building standards (i.e. using seismic force modification factors from national building codes) might be safe in some regions, but could be unsafe in regions where subduction interface events are possible.

ACKNOWLEDGMENTS

The study in this paper is part of the PhD dissertation of the first author which was funded by the Natural Sciences and Engineering Research Council of Canada (NSERC).

REFERENCES

- [1] Goldfinger, C., Nelson, C.H., Morey, A.E., Johnson, J.E., Patton, J.R., Karabanov, E., Gutierrez-Pastor, J., Eriksson, A.T., Gracia, E., Dunhill, G. and Enkin, R.J. (2012). *Turbidite event history: Methods and implications for Holocene paleoseismicity of the Cascadia subduction zone*. US Geological Survey Professional Paper, 1661.

- [2] Chandramohan, R., Baker, J.W. and Deierlein, G.G. (2016). "Impact of hazard-consistent ground motion duration in structural collapse risk assessment". *Earthquake Engineering and Structural Dynamics* 45(8), 1357-1379.
- [3] Chandramohan, R., Baker, J.W. and Deierlein, G.G. (2016). "Quantifying the influence of ground motion duration on structural collapse capacity using spectrally equivalent records". *Earthquake Spectra* 32(2), 927-950.
- [4] Fairhurst, M., Bebmazadeh, A., and Ventura, C.E. (2019). "Effect of ground motion duration on reinforced concrete buildings". *Earthquake Spectra*. In press.
- [5] Raghunandan, M. and Liel, A.B. (2013). "Effect of ground motion duration on earthquake-induced structural collapse". *Structural Safety*, 41, 119-133.
- [6] National Research Council of Canada (NRCC). (2010). *National Buildings Code of Canada*, Ottawa, Ont., Canada.
- [7] McKenna, F., Fenves, G.L., Scott, M.H. and Jeremic, B. (2000). *Open System for Earthquake Engineering (OpenSees)*, Pacific Earthquake Engineering Research Center, Berkeley, Ca.
- [8] Pugh, J. (2012). *Numerical Simulation of Walls and Seismic Design Recommendations for Walled Buildings*, Doctoral Dissertation, University of Washington, Seattle, Wa.
- [9] Los Angeles Tall Building Structural Design Council (LATBSDC). (2017). *An Alternative Procedure for Seismic Analysis and Design of Tall Buildings Located in the Los Angeles Region*, Los Angeles, Ca.
- [10] Galano, L. and Vignoli, A. (2000). "Seismic behavior of short coupling beams with different reinforcement layouts". *ACI Structural Journal* 97(6), 876-885.
- [11] Lowes, L.N., Mitra, N. and Altoontash, A. (2004). *A Beam-column Joint Model for Simulating the Earthquake Response of Reinforced Concrete Frames*, PEER Report 2003/10. Pacific Earthquake Engineering Center (PEER), University of California, Berkeley, Ca.
- [12] Yassin, M.H.M. (1994). *Nonlinear Analysis of Prestressed Concrete Structures under Monotonic and Cyclic Loads*, Doctoral Dissertation, University of California, Berkeley, Ca.
- [13] Mander, J.B., Priestley, M.J. and Park, R. (1988). "Theoretical stress-strain model for confined concrete". *Journal of Structural Engineering*, 114(8), 1804-1826.
- [14] Brown, J. and Kunnath, S.K. (2000). *Low Cycle Fatigue Behavior of Longitudinal Reinforcement in Reinforced Concrete Bridge Columns*, NCEER Technical Report 00-0007, National Center for Earthquake Engineering Research, State University of New York at Buffalo, Buffalo, N.Y.
- [15] Zhao, J., and S. Sritharan. (2007). "Modeling of strain penetration effects in fiber-based analysis of reinforced concrete structures". *ACI Structural Journal*, 104(2), 133-141.
- [16] Lin, T., Haselton, C.B., and Baker, J.W. (2013). "Conditional spectrum-based ground motion selection. Part I: Hazard consistency for risk-based assessments". *Earthquake engineering and structural dynamics*, 42(12), 1847-1865.
- [17] NEHRP Consultants Joint Venture. (2011). *Selecting and Scaling Earthquake Ground Motions for Performing Response-History Analyses*. NISTGCR-11-917-15.
- [18] Halchuk, S., Allen, T.I., Adams, J. and Rogers, G.C. (2014). *Fifth generation seismic hazard model input files as proposed to produce values for the 2015 National Building Code of Canada*. Geological Survey of Canada, Open File, 7576.
- [19] Baker, J.W., and Jayaram, N. (2008). "Correlation of spectral acceleration values from NGA ground motion models". *Earthquake Spectra*, 24(1), 299-317.
- [20] Bebmazadeh, A., Fairhurst, M., and Ventura, C.E. (2017). "Correlation of spectral values in worldwide subduction zone earthquakes". In *16th World Conference on Earthquake Engineering*, Santiago, Chile.
- [21] Carlton, B., and Abrahamson, N. (2014). "Issues and approaches for implementing conditional mean spectra in practice". *Bulletin of the Seismological Society of America*, 104(1), 503-512.
- [22] Jayaram, N., Baker, J.W., Okano, H., Ishida, H., McCann Jr, M.W., and Mihara, Y. (2011). "Correlation of response spectral values in Japanese ground motions". *Earthquake and Structures*, 2(4), 357-376.
- [23] Jayaram, N., Lin, T., and Baker, J.W. (2011). "A computationally efficient ground-motion selection algorithm for matching a target response spectrum mean and variance". *Earthquake Spectra*, 27(3), 797-815.
- [24] Ancheta, T.D., Darragh, R.B., Stewart, J.P., Seyhan, E., Silva, W.J., Chiou, B.S., ... and Kishida, T. (2013). *Peer NGA-West2 database*. Pacific Earthquake Engineering Research Center (PEER), Berkeley, Ca.
- [25] Bebmazadeh, A., Ventura, C.E., and Fairhurst, M. (2015). "S²GM: A tool for ground motion selection and scaling". In *2015 Los Angeles Tall Building Structural Design Council Annual Meeting*, Los Angeles, Ca.
- [26] Kinoshita, S. (1998). Kyoshin Net (K-net), *Seismological Research Letters*, 69(4), 309-332.
- [27] Fairhurst, M., Bebmazadeh, A., and Ventura, C.E. (2019). "An algorithm for the development of hazard consistent record suites: example for subduction megathrust records". *Earthquake Spectra*. In press.
- [28] Seifried, A.E. (2013). *Response compatibilization and impact on structural response assessment*. Doctoral dissertation, Stanford University, Ca.
- [29] Hancock, J., Watson-Lamprey, J., Abrahamson, N.A., Bommer, J.J., Markatis, A., McCoy, E., and Mendis, R. (2006). "An improved method of matching response spectra of recorded earthquake ground motion using wavelets". *Journal of Earthquake Engineering*, 10(1), 67-89.